Proceedings of the 1st Global Power and Propulsion Forum
GPPF 2017
Jan 16-18, 2017, Zurich, Switzerland
www.pps.global

GPPF-2017-33

MULTI-OBJECTIVE OPTIMISATION OF A CENTRIFUGAL COMPRESSOR FOR A MICRO GAS TURBINE OPERATED BY CONCENTRATED SOLAR POWER.

Davide Iaria
City, University of London
Iaria.davide@city.ac.uk
London, UK

Mahmoud Khader
City, University of London
Mahmoud.khader.1@city.ac.uk
London, UK

Jafar Alzaili
City, University of London
Jafar.alzaili@city.ac.uk
London, UK

Abdulnaser Sayma
City, University of London
a.sayma@city.ac.uk
London, UK

ABSTRACT

Solar powered micro-gas turbines (MGTs) are required to work over a wide range of operating conditions due to the fluctuations in the solar insulation. This means that the compressor has to perform efficiently over a wider range than in conventional MGTs.

To be able to extend the efficient operating range of a compressor at the design stage, both impeller blades and diffuser passage need to be optimised. Vaneless diffusers could offer more flexibility to extend the operating range than typical diffuser vanes.

This paper presents a methodology for the design and optimisation of a centrifugal compressor for a 6 kW micro-gas turbine intended for operation using a Concentrated Solar Power (CSP) system using a parabolic dish concentrator. Preliminary design parameters were obtained from the overall system specifications and detailed cycle analysis combined with practical constraints.

The compressor's geometry optimisation has been performed using a fast and computationally efficient method, which involves the Latin hypercube Design of Experiment (DoE) technique coupled with the response surface method (RSM) in order to build a regression model through CFD simulations. Three different RSM techniques were compared with the aim to choose the most suitable technique for this specific application and then a genetic algorithm was applied.

The CFD analysis for the optimised compressor showed that the high efficiency operating range has increased compared to the baseline design. Cycle analysis for the plant has been performed in order to evaluate the effect of the new compressor design on the system performance. The simulations demonstrated that the operating range of the plant was increased by over 30%.

INTRODUCTION

Solar power generation systems are environmentally friendly, have the potential to be economically feasible and provide a sustainable energy source.

Solar dish is one of the technologies available in the market, albeit not widely yet. Most of these systems have been developed with integrated Stirling engines which have demonstrated to be a complex and expensive system with poor reliability and difficulty to follow transient plant operations [18].

Optimised Micro Gas Turbine Solar Power (OMSoP) is a project funded by the European commission as a part of its contribution to CO_2 emission reduction. The OMSoP project aims to demonstrate the feasibility of a Solar dish CPS plant, powering a micro gas turbine (MGT).

Gas turbines typically have relatively high design point efficiency but with significant reduction at off-design conditions. Fluctuation of the solar flux during the day can cause the machine to work in off design conditions with a significant reduction of the MGT's performance.

One contributor to this behaviour of the MGT is the compressor characteristics where efficiency at a given rotational speed has a sharp peak. A compressor with less variation in efficiency over a wide range of mass flow rates and rotational speeds can help to improve the off design performance of the MGT. The selection of the most suitable diffuser in this context is important. In this study, it was postulated that a vaneless diffuser could be a good compromise between high design point efficiency and uniform characteristics.

To obtain the best performance an optimisation problem must be solved in order to obtain a suitable geometry for the given design specifications. An optimisation is a process,

which aims to find the optimal solution of a problem and can consist of a single or multiple objectives. During the optimisation process, the evaluation of the solution can require hours, or even days of CPU time, to produce results. From this point of view using a fitness approximation can improve the computational efficiency especially in cases where the model is complicated and the relationship between variables is highly non-linear.

As explained by Cavazzuti [5], in order to perform a reliable and computationally cheap response surface approximation, a design of experiment (DOE) is necessary. DOE is generally coupled with the Response Surface Method (RSM or meta-model), which can interpolate or approximate the information obtained from a numerical simulations (or experiments) in an approximated function.

The choice of the response surface is one of the most important factors in this optimisation procedure and there is plentiful of regression and statistical models available in the literature for this application. Khalfallah et al [16] performed a blade-shape optimisation procedure starting from the blade-shape parameterization through B-spline techniques. Then CFD simulations were used to evaluate the output parameters in the design space, and then, a radial basis function (RBF) RSM model was used to approximate the function. Finally, the genetic algorithm NSGA-II was applied to produce the optimal Pareto front.

Guo et al. [12] performed a multi-objective optimisation of a mini turbojet engine using a second order polynomial RSM. Starting from an initial compressor the RSM was coupled with a DOE and a fast optimisation was performed to get the maximum efficiency and the maximum pressure ratio. The same approach was used by Zhang et al. [26] using an optimisation technique that involves a DOE, an artificial neural network (ANN) RSM and a NSGA-II genetic algorithm with the aim to maximise the efficiency of an helico-axial pump.

Another powerful method to generate an output variable for given inputs is the Kriging meta-model. Kriging was originally used in the field of the geostatistics, but can be applied to a turbomachinery problem. Zhang et al. [28] optimised a double suction centrifugal pump training a Kriging RSM through a Latin hypercube DOE and then applying a genetic algorithm.

In this study, design and optimisation of a centrifugal compressor for solar application has been performed. The optimisation problem is solved through a response surface optimisation. The DOE space filling is obtained through a Latin Hypercube, while the RSM has been chosen as the most accurate and fast between three different methods: Full second order polynomial, artificial neural network and Kriging. Following an iterative process for the surface training, a genetic algorithm has been applied to find the best solution or the best trade-off between the objectives.

METHODOLOGY

Compressor design specifications

In the first part of this work, a centrifugal compressor was designed for a recuperated micro gas turbine for solar applications. The plant's schematic layout is shown in Figure 1. The main components of the MGT are: compressor, recuperator, and turbine. The solar irradiation is focused on a receiver using a parabolic dish, which transfers the heat to the MGT working fluid. The micro gas turbine net output power is 6 kWe and has the component specifications listed in Table 1.

Table 1. Micro-gas turbine components design point specifications

Parameter	value
Compressor efficiency	74%
Turbine efficiency	80%
Recuperator effectiveness	85%
Receiver efficiency	80%
Electrical efficiency	90%

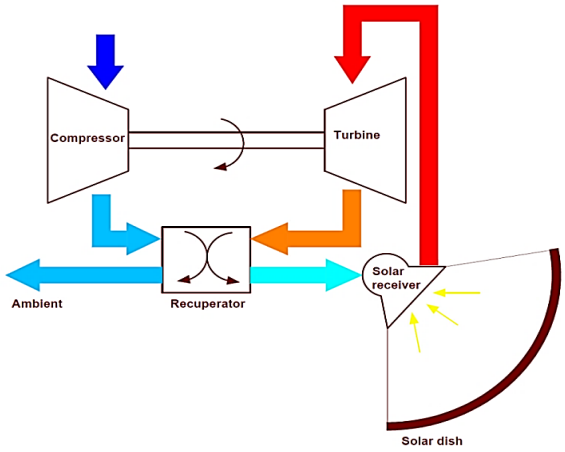

Figure 1.Solar powered Recuperated Micro turbine scheme.

A cycle analysis, considering a turbine entry temperature $TIT = 1173\ K$, was performed for a wide range of pressure ratios, rotational speeds and mass flow rates. Results have shown that the maximum achievable cycle efficiency is for a compressor pressure ratio of 3, rotational speed of 130 krpm and mass flow rate 0.09 kg/s.

Compressor design process

Centrifugal compressor design procedures are well documented in the literature [13], [24]. Using these methods a 1D design tool has been built. The output geometrical parameters were used to generate the blade and splitter geometry using a commercial tool (ANSYS BladeGen). The geometry of the blades was defined by the hub and shroud curves that define the camber angles θ at meridional planes, the exit angle β and the blade thickness in the radial direction. Where θ is the blade angle distribution referred to the meridional plane.

In this study both vaneless and vaned diffusers were designed, the first was designed as a simple passage made by

parallel walls, while the vaned diffuser was designed as a wedge type. Views of the vanless compressor (a) and compressor and diffuser are shown in Figure 2

The main design parameter are reported in table 2.

Table 2. Compressor's main design parameter.

Hub radius	9 mm
Inlet height	9.5 mm
Number of blades	8
Number of splitter	8
Impeller tip width	2.4 mm
Impeller tip radius	31.9 mm

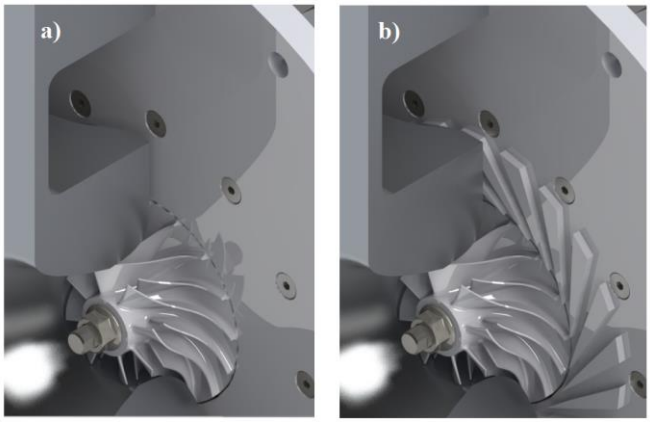

Figure 2. Cutaway of the vaneless (a) and vaned (b) diffuser compressors resulting from the design procedure.

Numerical Method

The computational domain consists of the diffuser, impeller and splitter passages. Given the high number of CFD simulations needed to build an accurate response surface, the O-H grid type mesh, generated using ANSYS TurboGrid, was used for the analyses. A grid independence study was performed in order to find a good compromise between simulation accuracy and computational effort. The selected number of grid points for the vaned diffuser compressor was around 920,000, while for the vaneless diffuser mesh, given its geometrical simplicity, had around 350,000.

The solid walls were treated as adiabatic boundaries with non-slip condition applied and the effect of the tip clearance (4%) has been considered.

The numerical simulations were carried out using the RANS based solver within ANSYS CFX. The turbulence model used was the two-equation Hybrid (shear stress transport SST).

The Optimisation Process

A flow chart of the optimisation technique is shown in Figure 3. The technique is called response surface optimisation and generates an approximated function that can be used to find a set of geometrical parameters that maximise the compressor efficiency. Starting from the initial compressor, the first step was to select the variables (or parameter) influencing the optimisation process, the input and output parameters. Input geometrical parameters are needed to fully characterise the problem from the design point of view, but it should be taken into consideration that the complexity of an optimisation problem increases exponentially with the number of parameters. The output variables, resulting from the solution of CFD simulations, are functions of the input parameters. These parameters give information about the problem and are the variables to be maximised during the optimisation

A significant number of training points are needed to build the surface. To achieve the maximum accuracy with the minimum number of samples a DOE technique was used to generate the training database. CFD simulations were used to evaluate the output variables for each point of the database.

The DOE was then coupled to a RSM to approximate the behaviour of the system in the design space. The advantage of using a DOE with a RSM technique is that it is easy to apply an optimisation algorithm on it. The drawback is that it is still an approximation, and its accuracy depends on the number of training points used to generate the surface. To overcome this issue an iterative approach was applied:

1. Apply a DOE+RSM technique.
2. Run a response-surface-based optimisation.
3. Simulate the optimisation candidate points with CFD analysis.
4. Add the new samples to the DOE database.
5. Update the RSM and repeat until the accuracy of the surface meet the requirements.

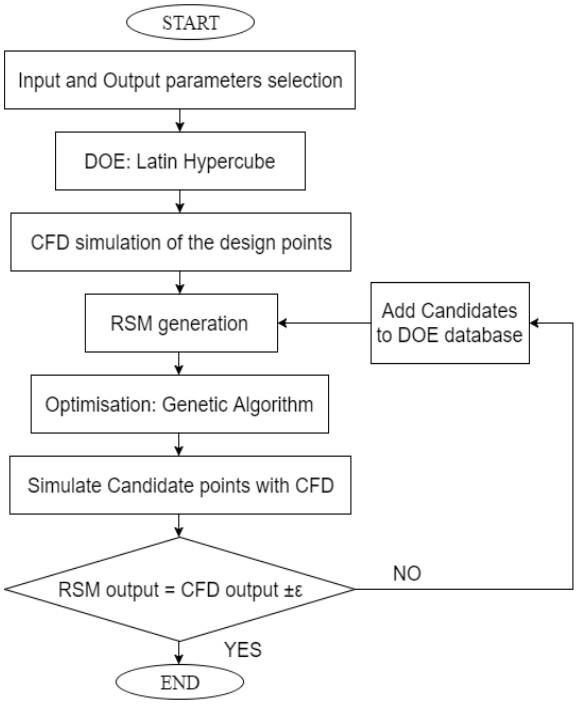

Figure 3. Flow chart of the optimisation technique.

The DOE technique used in this work is called *Latin Hypercube DOE*. Latin Hypercube uses a statistical approach to generate random training points (or samples) for each

parameter. The design space of each variable *M* is subdivided into *N* intervals of the same length, generating a matrix. The samples are chosen in these intervals, in such a way that each row and each column of the matrix are not selected twice. Different techniques are available to select the training points in the matrix, in this paper an orthogonal sampling scheme was used and all the samples were chosen simultaneously subdividing the intervals *N* into *N* sub-volumes. The selection process was performed by choosing the same amount of training points randomly from each of the sub-volumes.

In this work, the ANSYS DesignXplorer tool was used to compare the different RSM techniques were in order to select the meta-model that can guarantee the highest accuracy with the minimum computational cost. Among all the available techniques in ANSYS, the most suitable for a multi-objective optimisation with a genetic algorithm are the three described below.

The first technique is the *Standard full second order polynomial***;** a regression technique which determines the relationship between the input and the output parameters with a second order polynomial trend line.

The second technique is the *Kriging* algorithm, which computes a weighted average of the known values of the function in the neighbourhood of the point to be estimated. The output value $\hat{Z}$ in equation 1, is a linear combination of weighting factors (w_i) and known input point values (Z_i).

$$\widehat{Z} = \sum_{i=0}^{n}(w_i * Z_i)\,. \qquad (1)$$

The third technique is a *Neural Network* or *Artificial Neural Networks* (ANN). The optimisation process is divided into two different phases: the diffuser optimisation and the rotor blade-shape optimisation.

Vaneless Diffuser Optimisation

Both vaned and vaneless diffusers were designed and compared, although, given its comparative better performances at off-design conditions, the vaneless diffuser was selected for the further optimisation. The absence of vanes in the diffuser results in a compressor in a wide range of working points eliminates the incidence loss at the inlet of the vanes. Nevertheless, a vaneless diffuser sometimes can't ensure the recovery of all the kinetic energy in the flow, and the length of the diffuser must increase to get the right exit velocity. However, the more the diffuser length increases the more there is pressure drop and the optimal solution have been chosen looking for a compromise between the Total-to-Total and Total-to-Static efficiencies.

Table 3. Input parameters design space for the vaneless diffuser optimisation.

Parameter	Lower Bound	Upper Bound
Tip width	2 mm	2.6 mm
Diffuser length	20 mm	30 mm
Diffuser exit width	1.5 mm	2.6 mm

The input parameters and their respective design space are shown in Table 3. The are two main geometrical parameter for a vaneless diffuser: the diffuser length and the diffuser exit width. In addition, the impeller tip width was selected since it controls the mass flow passing through the impeller exit as the blade exit angle is fixed. This is important since the constraints of the optimisation are a mass flow of $0.09\ kg/s$ and a total pressure ratio of three, thus a small design space for the tip width parameter was selected.

For the other two parameters, a relatively large variation range was selected in order to explore a wider design space. The lower bound of the diffuser length was selected as it corresponds to the minimum allowed kinetic energy recovery the upper bound corresponds to the maximum allowed pressure drop. For what concern the diffuser exit width, usually is a good design practice to keep its value smaller or equal to the tip width. For this reason, the upper bound corresponds to the tip width upper bound. Moreover to ensure that the diffuser exit width is smaller or equal to the tip width, a constraint has been imposed to the optimisation problem.

In order to obtain a near-flat efficiency curve, the objective has been set to maximise the efficiency, both Total-to-Static and Total-to-Total, in the design point (DP) and two more points in its neighbourhood, distinguished by different exit static pressure, as shown in Equation 2. The design point has an exit static pressure of 2.5 atm, while the other pressures are 2.3 atm and 2.8 atm.

$$Maximise \begin{cases} \eta_{TS}(DP); \\ \eta_{TT}(DP); \\ \eta_{TS}(2.3); \\ \eta_{TT}(2.3); \\ \eta_{TS}(2.8); \\ \eta_{TT}(2.8); \end{cases} \qquad (2)$$

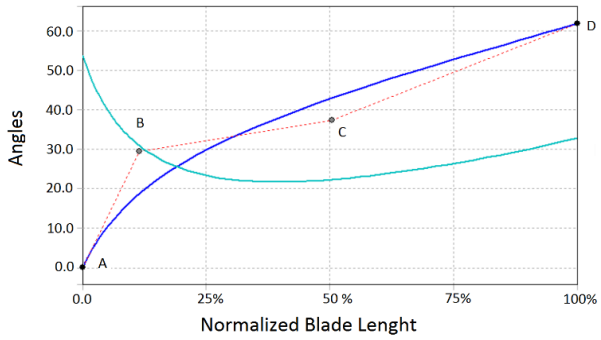

Figure 4. The θ angle is represented in blue and the β exit flux angle is represented in cyan; both are function of the normalised blade length.

Impeller Blade-Shape Optimisation

In the second optimisation the input parameters are the ordinate coordinates of the spline, which defines the blade shape as shown in Figure 4. Where the angle θ, is the blade camber angle referred to a meridional plane and the β exit flux angle, is the blade exit angle; both are functions of the normalised blade length. The curve chosen is a cubic Bezier spline defined by four points A, B, C and D. The parametric equation for a cubic Bezier curve is reported in Equation 3.

$$b(t) = A(1-t)^3 + 3B\,t(1-t)^2 + 3C\,t^2(1-t) + D\,t^3$$
$$\text{with } t \in [0,1]. \qquad (3)$$

The spline was generated with only four control points otherwise, with higher number of control points, the random approach of the DOE can generate invalid blade shapes. The parameters are the B, C, D-y coordinates for the meridional distribution of the camber angle at the hub, and the B and C y-coordinates for the shroud.

The A y-coordinates was fixed to zero for both the camber lines, indeed if this value changes the inlet blade angle would also change. The D-y coordinate at shroud was imposed to be equal to the D-y coordinate with one less input parameter and then less training points to be simulated, decreasing from 90 to 50.

The variation range of the input parameter is reported in Table 4 in terms of angle θ . The angle β was not considered as an input parameter since it is directly related to θ.

Table 4. Input parameters variation range for the blade-shape optimisation.

	B hub	C hub	D hub	B shroud	C shroud
Lower bound	29°	34°	60°	30°	39°
Upper bound	33°	38°	64°	34°	43°

Concerning the output parameters, very little has changed from the first optimisation of the diffuser. In this case, there is no trade-off between η_{TT} and η_{TS} and the objective function was set as:

$$Maximise \begin{cases} \eta_{pTT}(DP); \\ \eta_{pTT}(2.3); \\ \eta_{pTT}(2.8); \end{cases} \qquad (4)$$

The same constraints on the mass flow and the pressure ratio were kept at the design point for the second optimisation.

The optimisation algorithm used in this work was a Multi-Objective Genetic Algorithm (MOGA) implemented in ASNYS. Typical parameters to evaluate the convergence of a MOGA are the convergence stability percentage and a maximum allowable Pareto percentage. The first represents the stability of the population in the current generation and the typical value of 2% was considered. The second is the ratio between the number of points on the Pareto front and the number of samples in the current generation, in this case the value considered for the converge was 80%.

RESULTS AND DISCUSSION

The first step was to understand which RSM is more suitable for this application. For this reason a comparison between three different RSM technique was performed. This showed that the Kriging meta-model is the best in term of accuracy and number of design points needed for a good fit. Figure 5 shows for Kriging a chart named "goodness of fit", the charts compare a normalised value of CFD (observed) results and the results from the RSM (predicted). The best results can be obtained when the point is on the bisector.

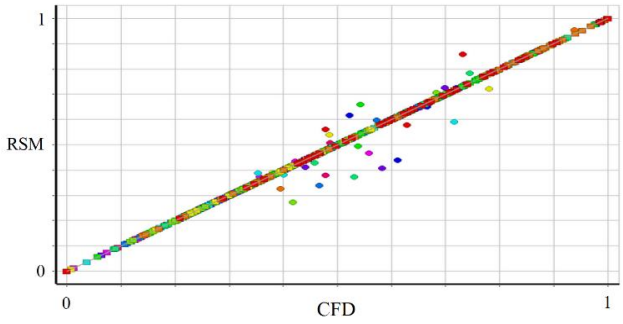

Figure 5. Kriging RSM goodness of fit.

A database with 35 design points and 15 verification points was built. Six output variables correspond to each point, each output variable can be distinguished by different colours in Figure 5. Statistical analysis for the Kriging RSM showed that the root mean square error was around 0.5% for each output variable, while the other two techniques can't guarantee a value lower than 5%. For this reason the Kriging RSM was selected as the function approximation technique to be used in the optimisation.

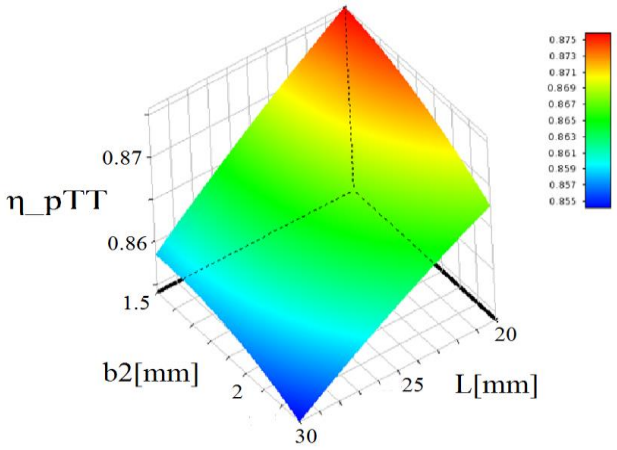

Figure 6. Kriging response surface example. Total to total polytrophic stage efficiency at Design point as a function of the tip width (b2) and the diffuser length (L).

Diffuser Optimisation

Once the response surface technique has been defined, the RSM was built and the optimisation was performed. The response surface shows the inter-dependence between the stage efficiency and the geometric parameters.

As shown in Figure 6, the longer the diffuser length is the more the pressure losses are, as expected, leading to a lower Total-to-Total efficiency. In the meantime a higher exit kinetic energy recovery can be ensured and then a higher Total-to-

Static efficiency. This behaviour can be easily verified by inspection of Figure 7, where the Pareto fronts of the optimisation problem are plotted, each Pareto front belongs to a successive iteration and is distinguished by different colours. The multidimensional characteristic of the problem and the choice of finding the training points for the response surface between the optimal solutions of a lower level RSM, lead to a shape that cannot be defined as usual Pareto front. Despite this, it is clear in the trend between these two objectives.

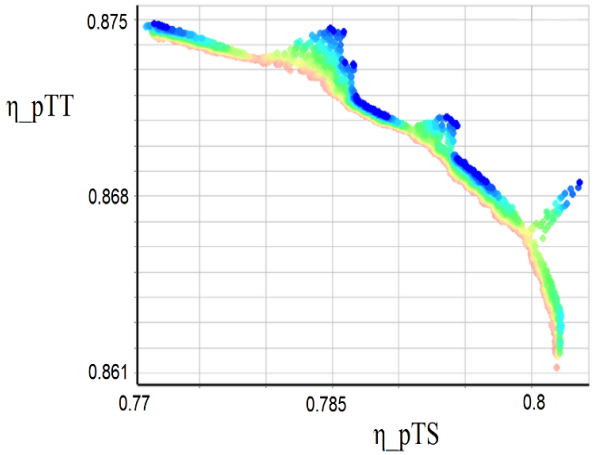

Figure 7. Bi-dimensional section of the Pareto front.

Some of these points were selected and evaluated using CFD. One of those was chosen as the candidate point for the next optimisation. Further geometry details are given in Table 5.

Table 5. Optimized diffuser geometry

Tip Width	Diffusor Length	Diffusor exit Width
2.01	27.52	1.94

Figure 8 shows that the optimised vaneless diffuser results a wider range of working points with high efficiency that is more than twice the operating range of the original compressor with vaned diffuser. The drawback is that the highest efficiency that can be reached by the compressor has reduced, which is also to be expected.

The maps are calculated for a rotational speed of 130 krpm, an inlet temperature $T_{01} = 298\ K$ and an inlet pressure of 101,325 Pa .

Blade-Shape Optimisation

The second optimisation aimed at improving the blade-shape in an attempt to recover the loss of peak efficiency. In this case, there is no trade off to be faced. The optimisation must be considered in any case as multi-objective, as the Kriging RSM considers any variable as independent from the others.

Figure 8 shows a characteristic curve of the optimised compressor. The curve shows a comparison of the compressors resulting from the first and the second optimisation with the previously designed vaned diffuser compressor.

The second optimisation led to improvement in the performances of the compressor and the CFD analysis demonstrates that optimising the blade-shape could significantly extend the range of high efficiency working points, improving in the meantime the maximum efficiency.

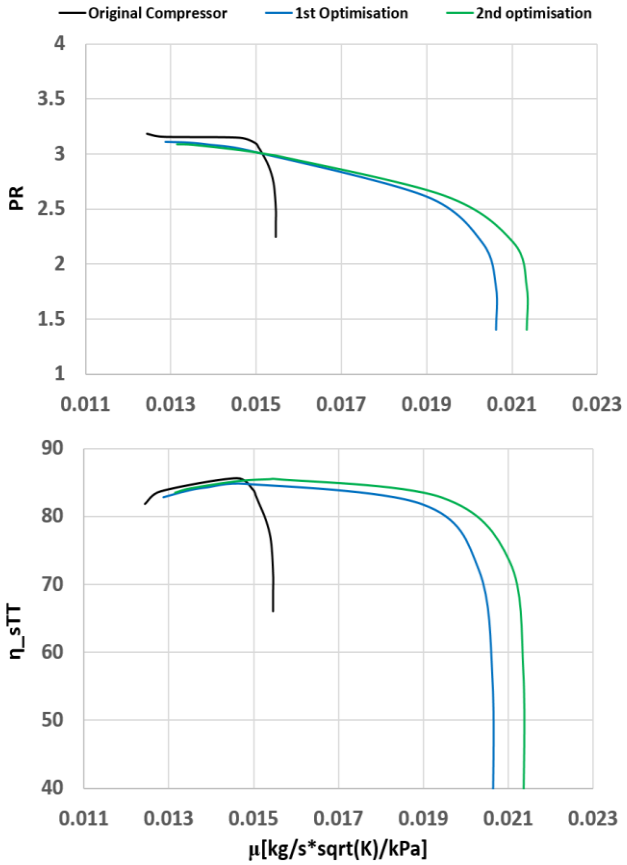

Figure 8. 130 krpm characteristic maps for the orginal vaned diffuser compressor (black) optimised vaneless diffuser compressor (blue) and the optimised blade-shape compressor (green).

The shape of the blade has been clearly modified as shown in Figure 9, where the original blade is represented in green and the optimised blade in grey.

Plant part-load analysis

As already mentioned, extending the compressor's working range with high efficiency can help to improve the whole plant performances at off-design condition. In order to verify the effective plant performance boost, an off-design analysis was performed.

The plant was simulated using a cycle analysis model developed during this study that can calculate the off-design performances of the plant considering the main components characteristics and limits, as:

- $Compressor\ surge\ and\ choke\ limits.$
- $TIT_{MAX} = 1173\ K.$
- $n_{MAX} = 150\ krpm.$
- $T_{exhMAX} = 873\ K.$

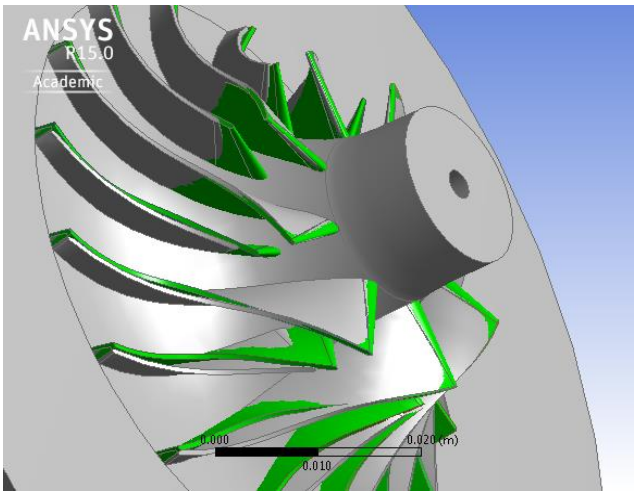

Figure 9. Comparison between the original (green) and the optimised blade (grey)

Figure 10 shows the thermo-dynamical efficiency of the plant as a function of the power output. As the power increases, the limitation on the TIT imposes a variation in the rotational speed, which is done using the control system.

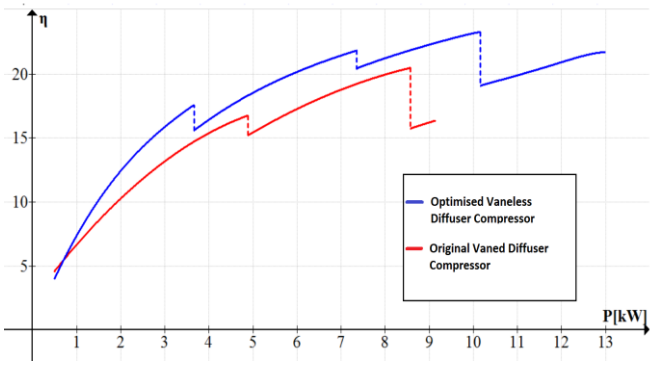

Figure 10. Thermodynamic cycle efficiency as a function of the power output. Comparison between the plant with the optimised compressor (blue) and the plant with the original vaned diffuser compressor(red)

For this reason, the curve is segmented. The steps on the curves represent the change in the rotational speed imposed to achieve the maximum TIT for the optimised compressor (blue line) and for the original compressor with vaned diffuser (red line).

The study shows that the operating range of the plant was extended by almost 30% increasing the overall efficiency of the plant. This is due to the different shape of the characteristic maps. The vaneless diffuser compressor can guarantee a high-pressure ratio for a high range of mass flows, resulting in a higher plant thermodynamic efficiency.

CONCLUSIONS

The design and optimisation of a centrifugal compressor for concentrated solar power applications was performed. The optimisation of the compressor was conducted by coupling DoE with RSM techniques and a genetic algorithm. The optimisation technique was demonstrated to be very fast and computationally efficient ant it can be developed even when little is known about the problem.

Starting from a parametric geometry analysis, two different optimisation processes were performed to optimise the diffusor main geometric parameters and the blade shape in order to obtain a centrifugal compressor with a higher operating range and high part load efficiency. The chosen DoE technique was the Latin hypercube, while the selected RSM was Kriging meta-model. After a careful comparison Kriging RSM demonstrated to guarantee the best approximation when compared to full second order polynomial and ANN, in term of speed of surface training and accuracy.

The optimised compressor, which was generated by the genetic algorithm, shows a wider range of high efficiency that is more than twice the original compressor with vaned diffuser. The drawback is a 0.5 % decrease of the peak stage efficiency. Moreover the off design analysis of the plant demonstrated that the thermodynamic efficiency has increased, and the power range was extended by over 30%.

NOMENCLATURE

$b_2 = Blade\ tip\ width;$

$L = Diffuser\ lenght;$

$\dot{m} = Mass\ Flow;$

$PR = Pressure\ Ratio;$

$\beta = Blade\ Exit\ angle;$

$\eta_{pTT} = Total - to - Total\ Polytrophic\ Efficiency;$

$\eta_{sTT} = Total - to - Total\ Isentropic\ Efficiency;$

$\eta_{pTS} = Total - to - Static\ Polytrophic\ Efficiency;$

$\eta_{sTS} = Total - to - Static\ Polytrophic\ Efficiency;$

$\theta = Camber\ angle\ on\ a\ meridional\ plane;$

$\mu = Corrected\ massflow\ \ m\sqrt{T_{01}}/p_{01};$

$TIT = Turbine\ Inlet\ Temperaure$

$T_{exh} = Turbine\ Exhaust\ Temperature;$

$n = Rotational\ speed;$

ACKNOWLEDGMENTS

The authors would like to thank Prof. Giovanni Cerri and the Fluid Machines department of Universitá degli studi di Roma3 for useful discussions and input to this work.

REFERENCES

[1] R. Abhari and M. Scheleer. Clearance effects on the evolution of the flow in the vaneless diffuser of a centrifugal compressor at part load condition. Journal of Turbomech, vol. 130, 2008.

[2] R. S. Abhari and S.-S. Hong. Effect of tip clearance on impeller discharge flow and vaneless

diffuser performance of a centrifugal compressor. Journal of Power and Energy, 2012.
[3] S. Anish and N. Sitaram. Computational investigation of impeller–diffuser interaction in a centrifugal compressor with different types of diffusers. IMechE Journal of Power and Energy,vol. 223, pp. 167-178, 2009.
[4] R. H. Aungier, Centrifugal Compressors: A strategy for Aerodynamic Design and Analysis, New York: ASME Press, 2000.
[5] M. Cavazzuti. Optimisation methods: From theory to the design. Springer Berlin Heidelberg 2013.
[6] Cho Soo-Yong, Kook-Young Ahn, Young-Duk Lee, Young-Cheol Kim. Optimal Design of a Centrifugal Compressor Impeller Using Evolutionary Algorithms. Mathematical Problems in Engineering, 01/2012, Volume 2012.
[7] A. Demeulenaere, Prof. Ch. Hirsch. Application of multipoint and multistage optimisation of the design of turbomachinery bades. 6th European Turbomachinery Conference, 2005.
[8] S. L. Dixon and C. A. Hall, Fluid Mechanics and Thermodynamics of Turbomachinery, USA: Elsevier, 2010.
[9] D. Eckardt. Instantaneous measurements in the jet-wake discharge flow of a centrifugal compressor impeller. ASME Journal of engineering power, pp. 337-346, 1975.
[10] M. R. Galvas. Analytical correlation of centrifugal compressor design geometry for maximum efficiency with specific speed. NASA, Washington, 1972.
[11] L.M. Gao, S.J. Wang and G. XI, Influence of Tip Clearance on the Flow Field and Aerodynamic Performance of the Centrifugal Impeller. Chines Journal of Aeronautics, vol. 15, 2002.
[12] S. Guo, Fei Duan, Hui Tang, Seng Chuan Lim, Mee Sin Yip. Multi-objective optimisation for centrifugal compressor of mini turbo jet engine. Aerospace Science and Technology, Volume 39, December 2014, Pages 414-425.
[13] D. Japikse, Centrifugal Compressor Design, Concepts Eti, 1996.
[14] Y. Jung, M. Choi, S. Oh and J. Baek. Effects of a non-uniform tip clearance profile on the performance and flow field in a centrifugal compressor. International Journal of Rotating Machinery, vol. 2012, p. 11, 2012.
[15] Y.-S. Kang, H.-J. Emu and S.-H. Kang. Tip clearance effect on through-flow and performance of a centrifugal compressor. KSME International Journal, vol. 18, pp. 979-989, 2004.
[16] S.Khalfallah, A Ghenaiet. Shape optimisation of a centrifugal compressor impeller. December 2013
[17] J.H.Kim, J.H. Choi, A. Husain, K.Y. Kim. Multi-objective optimization of a centrifugal compressor impeller through evolutionary algorithms. Proceedings of the Institution of Mechanical Engineers, Part A: Journal of Power and Energy, 01/2010, Volume 224, Issue 5.
[18] M. Lanchi, M. Montecchi, M. Adio, M. Falchetta. Investigation into the coupling of Micro Gas Turbine with CSP technology: OMSoP project. Energy Procedia 2015.
[19] A. Matta, M. Pezzoni, Q. Semeraro. A Kriging-based algorithm to optimize production systems approximated by analytical models. J Intell Manuf 2012.
[20] C. Rodgers. 5-25 kWe Micro-Gas turbines design aspects. ASME TURBOEXPO, Munich, 2000.
[21] C. Rodgers. Microturbine Rotational Speed Selection. ASME TURBOEXPO, San Antonio, 2013.
[22] J. Schiffmann, D. Favrat. Design, experimental investigation and multi-objective optimisation of a small-scale radial compressor for heat pump applications. Energy, 2010, Volume 35, Issue 1
[23] Y. Wei, Ruofu Xiao. Multiobjective Optimisation Design of a Pump–Turbine Impeller Based on an Inverse Design Using a Combination Optimisation Strateg. Journal of Fluids Enginering Vol. 136(1), 014501 (October 2013).
[24] A. Whitefield and N. C. Baines, Design of Radial Turbomachines, John Wiley, 1990.
[25] A. Whitefield. Preliminary design and performance prediction techniques for centrifugal compressors. Journal of Power and Energy, 1990.
[26] Zhang Jinya, Hongwu Zhu, Chun Yang, Yan Li, Huan Wei. Multi-objective shape optimisation of helico-axial multiphase pump impeller based on NSGA-II and ANN. Energy Conversion and Management, Volume 52, Issue 1, January 2011, Pages 538-546.
[27] Y. Zhang, Wu Jinglai, Zhang Yunqing, Chen Liping. Design Optimization of Centrifugal Pump Using Radial Basis Function Metamodels. Advances in Mechanical Engineering (2014)
[28] Y. Zhang, Sanbo Hu, Jinglai Wu, Yunqing Zhang, Liping Chen. Multi-objective optimisation of double suction centrifugal pump using Kriging meta-models. Advances in Engineering Software, Volume 74, August 2014, Pages 16-26.